Channel-Opening Kinetics of GluR6 Kainate Receptor†

Gang Li,‡ Robert E. Oswald,§ and Li Niu*,‡

Department of Chemistry, Center for Neuroscience Research, University at Albany, State University of New York, Albany, New York 12222, and Department of Molecular Medicine, Cornell University, Ithaca, New York 14853

Received May 15, 2003; Revised Manuscript Received August 15, 2003

ABSTRACT: GluR6 is an ionotropic glutamate receptor subunit of the kainate subtype. It plays an essential role in synaptic plasticity and epilepsy. We expressed this recombinant receptor in HEK-293 cells and characterized the glutamate-induced channel-opening reaction, using a laser−pulse photolysis technique with the caged glutamate (γ-*O*-(α-carboxy-2-nitrobenzyl)glutamate). This technique permits glutamate to be liberated photolytically from the caged glutamate with a time constant of ∼30 μs. Prior to laser photolysis, the caged glutamate did not activate the GluR6 channel, nor did it inhibit or potentiate the glutamate response. At the transmembrane voltage of −60 mV, pH 7.4 and 22 °C, the channel-opening and -closing rate constants were determined to be $(1.1 \pm 0.4) \times 10^4$ and $(4.2 \pm 0.2) \times 10^2$ s^{-1}, respectively. The intrinsic dissociation constant of glutamate and the channel-opening probability were found to be 450 ± 200 μM and 0.96, respectively. These constants are derived from a minimal kinetic mechanism of the channel activation involving the binding of two glutamate molecules. This mechanism describes the time course of the open-channel form of the receptor as a function of glutamate concentration. On the basis of the channel-opening rate constants obtained, the shortest rise time (20−80% of the receptor current response) or the fastest time by which the GluR6Q channel can open is predicted to be 120 μs. The open-channel form of the receptor determines the transmembrane voltage change, which in turn controls synaptic signal transmission between two neurons. The comparison of the channel-opening kinetic rate constants between GluR6Q and $GluR2Q_{flip}$, reported in the companion paper, suggests that at a glutamate concentration of 100 μM, for instance, the integrated neuronal signal will be dominated by a slower GluR6Q receptor response, as compared to the $GluR2Q_{flip}$ component.

GluR6 is an ionotropic glutamate receptor subunit of the kainate subtype (*1*, *2*). It can form homomeric receptor channels when expressed in heterologous expression systems such as human embryonic kidney (HEK-293) cells (*3*). GluR6 undergoes mRNA editing at the Q/R (glutamine/arginine) site located in membrane domain 2 (*4*), which is believed to line the channel pore of the receptor (*5*−*7*). The mRNA editing at this site is known to affect the GluR6 properties dramatically. The presence of R at this site decreases the channel permeability to calcium (*4*, *8*), reduces the mean conductance of the GluR6 channel by about 25-fold (*9*), and alters the current−voltage relationship from inwardly rectifying to linear or slightly outwardly rectifying (*4*, *10*). Furthermore, the extent of Q/R editing is developmentally regulated in that GluR6 is unedited embryonically, but the editing rises to ∼70−85% by birth (*11*). In addition, the disruption of GluR6 editing increases the vulnerability to seizures, suggesting that unedited GluR6 may contribute to the seizure generation (*12*). More recently, GluR6 has been implicated in other neurological conditions including schizophrenia (*13*) and Huntington's disease (*14*).

The opening and closing of the GluR6 receptor channel is presumed to occur in the submillisecond (ms) time scale. This is based, at least in part, on the lifetime of the open channel characterized by single-channel studies using domoate (domoate is a neurotoxin that can activate the kainate receptor channel but produces nondesensitizing currents) (*15*). However, the lifetime of the open channel has not been reported using the natural neurotransmitter glutamate. The binding of glutamate to its ion-channel receptors, including GluR6, is known to induce rapid receptor desensitization within milliseconds, a reaction that leads to the closure of the channel with the neurotransmitter bound (*16*). Therefore, a kinetic investigation of the receptor-channel opening requires the use of a kinetic technique with at least a submillisecond time resolution (*17*−*20*). Commonly used fast solution-exchange methods have not offered a time resolution high enough to resolve the rapid channel opening, occurring in the microsecond (μs)-to-ms time domain, from the rapidly ensuing channel desensitization. By these techniques, generally, the diffusion of ligands toward the surface of a cell or a patch of membrane and the mixing of ligands with the sites of the receptor is slow, as compared to the rate of the receptor-channel opening. Consequently, the

† This work was supported in part by grants to L.N. from the American Heart Association (0130513T), the Amyotrophic Lateral Sclerosis Association, and the Muscular Dystrophy Association. R.E.O. was supported by an NSF grant (IBN 9974604 and IBN 0323874). G.L. was supported by a postdoctoral fellowship from the Muscular Dystrophy Association.

* To whom correspondence should be addressed. Telephone: (518) 442-4447. Fax: (518) 442-3462. E-mail: lniu@albany.edu.

‡ SUNY−Albany.

§ Cornell University.

10.1021/bi034797t CCC: $25.00
Published on Web 10/01/2003

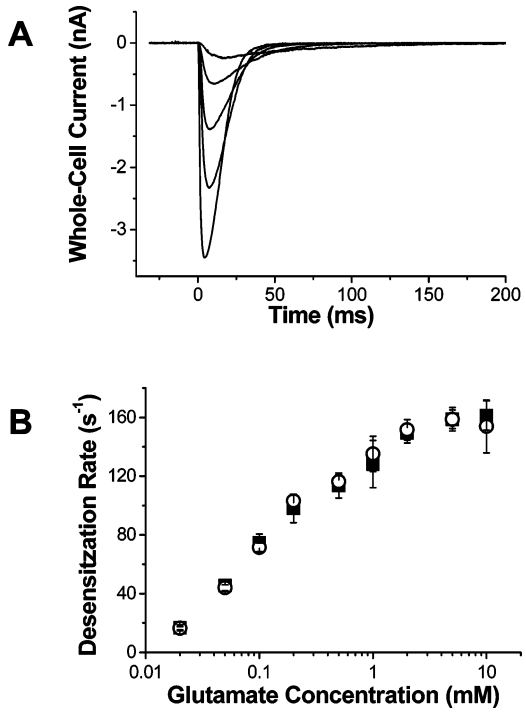

FIGURE 1: (A) Whole-cell currents measured from a HEK-293 cell. The currents were generated at time zero when glutamate was applied at the concentration, from bottom up, of 500, 200, 100, 50, and 20 μM, respectively. (B) Dependence of the desensitization rate constants on glutamate concentration. The open symbol represents the measurements from the HEK-293 cells expressing only GluR6Q, whereas the solid squares are from the measurements with the HEK-293 cells expressing both GluR6Q and GFP.

kinetics of the GluR6-channel opening is not well-understood.

Here, we use the laser−pulse photolysis technique (*17*−*19*, *21*) that employs *γ-O*-(α-carboxy-2-nitrobenzyl)glutamate (αCNB glutamate)[1] or caged glutamate (*22*). The caged glutamate is a photolabile precursor of glutamate. The caged glutamate and its photolytic side products are biologically inert as previously tested with rat hippocampal neurons (*22*), which is further confirmed with the GluR6 receptor in the present study. In kinetic experiments described next, caged glutamate is first equilibrated with the cell expressing the receptor and then photolyzed by a laser pulse. Free glutamate is released with a time constant of ~30 μs (*22*). Using this technique, we have characterized, and report here, the kinetic mechanism for the channel-opening reaction of the GluR6Q receptor channel, prior to receptor desensitization. The biological implications of the present study, in the context of the results using $GluR2Q_{flip}$ presented in the companion paper, are further discussed.

MATERIALS AND METHODS

Expression of cDNA and Cell Culture. The cDNA encoding GluR6Q was kindly provided by Prof. Steve Heinemann (Salk Institute). The plasmid was propagated in an *E. coli* host (DH5α) and purified using a kit from QIAGEN (Valencia, CA). GluR6Q was transiently expressed in HEK-293 cells using a standard calcium phosphate protocol (*23*). The cells were cultured in Dulbecco's modified Eagle's medium supplemented with 10% fetal bovine serum, 50 U/mL penicillin, and 50 μg/mL streptomycin from GIBCO/BRL (Carlsbad, CA) and maintained in a 37 °C, 5% CO_2, humidified incubator.

Unless otherwise noted, the HEK-293 cells were also transiently cotransfected with a plasmid harboring the green fluorescent protein (GFP) gene. The weight ratio of the plasmid expressing GFP to that expressing GluR6Q was 1:5. The amount of the GluR6Q used for transfection was 2−4 μg/35 mm culture dish. The GFP plasmid was a generous gift from Prof. Ben Szaro from SUNY−Albany. All transfected cells were used 48 h after the introduction of the expression plasmid(s).

Whole-Cell Current Recording. The procedure of the whole-cell recording was described in detail in the companion paper. Briefly, the resistance of the recording electrodes was ~3 MΩ when filled with the electrode solution. The electrode solution contained (in mM) 110 CsF, 30 CsCl, 4 NaCl, 0.5 $CaCl_2$, 5 EGTA, and 10 Hepes (pH 7.4 adjusted by CsOH). The external bath solution contained (in mM) 150 NaCl, 3 KCl, 1 $CaCl_2$, 1 $MgCl_2$, and 10 Hepes (pH 7.4 adjusted by NaOH). The whole-cell current (*24*) was recorded using an Axopatch-200B amplifier at a cutoff frequency of 2−20 kHz by a built-in, eight-pole Bessel filter and digitized at a 5−50 kHz sampling frequency by a Digidata 1322A (Axon Instruments). pCLAMP 8 (Axon Instruments) was used for data acquisition.

Laser−Pulse Photolysis and Cell-Flow Measurements. The laser−pulse photolysis and the cell-flow device have been described in the companion paper (*25*). αCNB glutamate was dissolved in the external bath buffer and delivered to the cell using a cell-flow device. After the cell was equilibrated with caged glutamate for 250 ms, a laser pulse was delivered to liberate free glutamate. A Minilite II pulsed Q-switched Nd:YAG laser (Continuum, Santa Clara, CA) tuned by a third harmonic generator was used to generate single laser pulses at 355 nm with a pulse length of 8 ns. The laser light was coupled into a fiber optic from Fiber-Guide Industries (Stirling, NJ), and the power was adjusted to be 200−800 μJ after coupling, detected by a Joulemeter from Gentec (Quebec, Canada).

The cell-flow device was used to deliver either caged glutamate for laser−pulse photolysis described previously or free glutamate to monitor the cell damage and to calibrate the concentration of photolytically released glutamate (*18*, *21*). Once a HEK-293 cell was in the whole-cell mode (*24*), it was lifted from the bottom of the dish and suspended in the external bath solution. The glutamate-induced whole-cell current was recorded as described previously (*25*). The amplitude was corrected for desensitization that occurred during the current rise by the method described in the companion paper.

All measurements were performed with cells voltage-clamped at −60 mV, pH 7.4, and room temperature. Each data point was an average of at least three measurements collected from at least three cells unless otherwise noted. Linear regression and nonlinear least-squares fitting (Levenberg−Marquardt algorithm) were performed using Origin 7. Uncertainties reported are the standard error of the fits.

[1] Abbreviations: AMPA, α-amino-3-hydroxy-5-methyl-4-isoxazolepropionic acid; αCNB glutamate, *γ-O*-(α-carboxy-2-nitrobenzyl)-glutamate; GFP, green fluorescent protein; NMDA, *N*-methyl-D-aspartate.

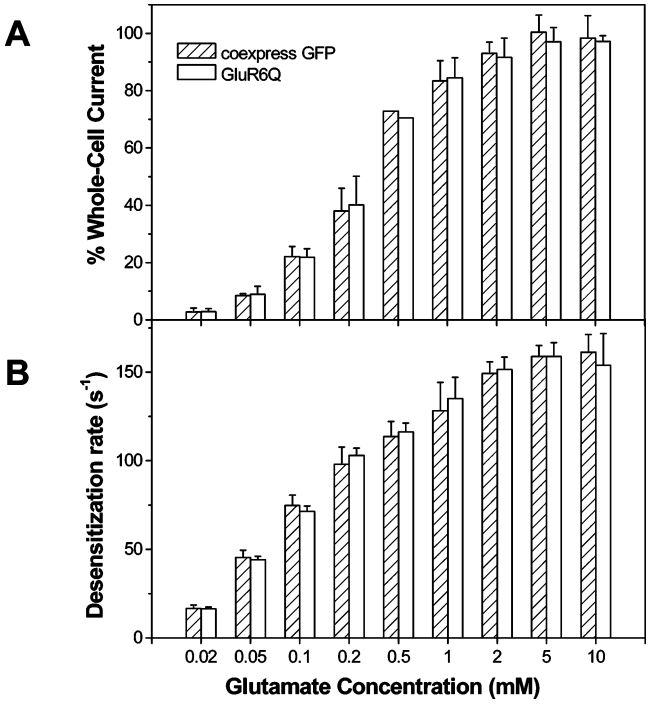

FIGURE 2: Coexpression of GFP in HEK-293 cells does not affect (A) relative current amplitudes and (B) desensitization rate constants for GluR6Q responses induced by glutamate. In panel A, the whole-cell currents from different cells were normalized to the current obtained at 0.5 mM glutamate, and the current amplitude at 10 mM was set to be 100%.

RESULTS

Glutamate-Induced Activation of GluR6Q. Figure 1A shows representative traces of the whole-cell currents evoked by glutamate. The current deviated from the baseline, at time zero, as a result of the opening of the receptor channels, and then returned toward the baseline due to desensitization or transient inactivation in the continued presence of glutamate. As a control, untransfected HEK-293 cells were tested with 10 mM glutamate (sufficient to saturate the receptor response, as seen in the dose−response plot in Figure 3), and no current was observed (data not shown). The desensitization process was adequately characterized by a first-order rate constant, which accounted for over 95% of the reaction. The observed desensitization rate constant increased with increasing glutamate concentrations but reached a plateau at ~2 mM, shown in Figure 1B. The profile of desensitization and the magnitude of the desensitization rate constants observed are all consistent with those obtained previously from either membrane patches (*26*, *27*) or lifted cells (*9*, *15*).

Coexpression of GFP with GluR6Q in HEK-293 Cells. Because of the characteristic green color, GFP was transiently coexpressed with GluR6Q in HEK-293 cells (see Materials and Methods) to facilitate the identification of single cells that might also express GluR6Q. To enhance the likelihood that a green cell also expressed GluR6Q, the GluR6Q plasmid was in excess relative to the GFP plasmid (see Materials and Methods). Under this condition, a linear correlation was observed between the intensity of fluorescence in a cell and the amplitude of the whole-cell current (data not shown). To demonstrate that the coexpression of GFP did not affect the function of GluR6Q, we examined two types of cells. One type expressed only GluR6Q, and the other expressed both GluR6Q and GFP. The desensitization rate constants

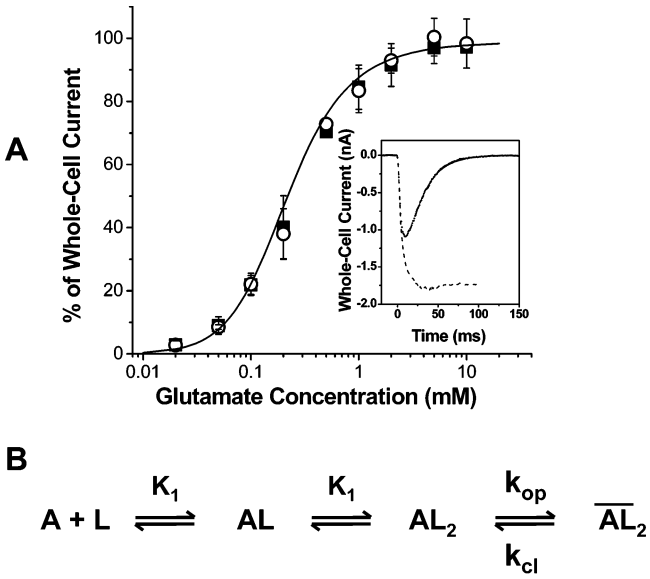

FIGURE 3: (A) Percentage of the whole-cell current as a function of glutamate concentration obtained in cell-flow measurements. Each data point is an average of at least three measurements from three cells. The whole-cell currents from different cells were normalized to the current obtained at 0.5 mM glutamate, and the current amplitude at 5 mM was set to be 100%. The current amplitude was corrected (see Materials and Methods and the companion paper), and an example is shown in the inset with the observed current amplitude (solid line) and the corrected one (dashed line). The open symbol represents the measurements from the HEK-293 cells expressing only GluR6Q, whereas the solid squares are from the measurements with the HEK-293 cells expressing both GluR6Q and GFP. The solid line is the nonlinear fit of the data based on eq 1. K_1 of 450 ± 200 μM, Φ of 0.12 ± 0.05, and $I_M R_M$ of 110 ± 10 were obtained. All symbols are defined in the text. (B) Minimum mechanism for the channel-opening reaction of GluR6 receptor. A represents the active, unliganded form of the receptor, L the ligand (glutamate), AL and AL_2 the ligand-bound closed channel forms, and $\overline{AL_2}$ the open-channel form of the receptor.

with and without GFP were the same at any given concentration of glutamate, shown in Figure 2B. Furthermore, the expression of GluR6Q in HEK-293 cells, judged by the relative current amplitude at any given concentration of glutamate, was statistically indistinguishable with and without GFP, shown in Figure 2A. As a control, the HEK-293 cells expressing only GFP showed no glutamate response even when tested with a 10 mM glutamate concentration. These results demonstrate that GFP, when expressed using a separate plasmid construct, can serve as an efficient and harmless cell marker for the study of GluR6Q in the HEK-293 cells.

Minimal Kinetic Mechanism and Equilibrium Constant for Channel Opening. The response of the GluR6 receptor in terms of the corrected current amplitude as a function of glutamate concentration or a dose−response relationship is shown in Figure 3A. In Figure 3A, the solid line is the best fit of the corrected current amplitudes at various glutamate concentrations, using eq 1.

$$I_A = I_M R_M \frac{L^2}{L^2 + \Phi(L + K_1)^2} \quad (1)$$

I_A represents the current amplitude at a given concentration of ligand, L is the molar concentration of the ligand, I_M is

the current per mol of receptor, and R_M is the number of mol of receptor in the cell. Φ^{-1} ($=k_{op}/k_{cl}$) is the channel-opening equilibrium constant. According to eq 1, the intrinsic dissociation constant of glutamate (K_1) was 450 ± 200 μM, and Φ 0.12 ± 0.05, respectively.

Eq 1 was derived based on a minimal kinetic mechanism for the channel opening, shown in Figure 3B. This is a general mechanism previously used to describe ligand-gated ion channels, including native glutamate receptors (*28*−*30*) and recombinant channels such as GluR6 (*26*) and GluR2 (*31*). The evidence that further supported this mechanism came from our analysis of the same dose−response relationship using the Hill equation (*32*, *33*). The Hill coefficient was 1.3 ± 0.1, consistent with the requirement of at least two bound glutamate molecules to open the channel. In AMPA receptors, for instance, the two-ligand binding model has been generally accepted, where the Hill coefficient ranges from 1.2 to 1.95 (*34*). It should be further noted that the assumption of binding of two glutamate molecules as a minimal number to open the channel does not argue against the proposed tetrameric composition (*35*−*37*). In addition, our analysis of the data (in Figure 3A) by the Hill equation yielded an apparent EC_{50} value (the concentration of ligand that produces 50% of the maximum activation) of 290 ± 11 μM. This value agrees with those previously reported, ranging from 200 to 762 μM for the GluR6Q homomeric channel expressed in HEK-293 cells (*26*, *27*, *38*, *39*). The K_1 value of 450 ± 200 μM, which represents the intrinsic equilibrium constant obtained from the model-dependent fitting (using eq 1), is qualitatively consistent with the EC_{50} values from not only our own data but previously reported data as well.

Biological Properties of Caged Glutamate Tested with GluR6Q in HEK-293 Cells. Previously, caged glutamate was found to be biologically inert when tested with glutamate receptors in rat hippocampal neurons (*22*). Hippocampal neurons were known to express endogenous kainate receptors (*28*, *30*), but it was unclear whether the density of GluR6Q was high enough to be sampled. Here, the biological properties of the caged glutamate (in the absence of a laser pulse to release free glutamate) were further tested with GluR6Q expressed in HEK-293 cells, using the cell-flow technique. In this experiment, the concentration of caged glutamate was chosen to be 2 mM, the highest used in the photolysis experiment shown next. On the other hand, the free glutamate used to evoke the receptor response was 200 μM and was near the highest concentration of the photolytically released glutamate in the laser−pulse photolysis experiments. Furthermore, the 200 μM glutamate chosen was near the K_1 value in the dose−response curve (Figure 3A), where it was the most sensitive region to detect any potential effect of the caged glutamate on the receptor response. That the glutamate-elicited receptor responses were identical in the presence and absence of caged glutamate, in Figure 4, judged by both the current amplitude and the desensitization rate, demonstrated that the caged glutamate did not activate the GluR6Q channel, nor did it inhibit or potentiate the glutamate response.

Kinetic Constants for Channel Opening. Using the laser−pulse photolysis technique that has a ~60 μs time resolution, together with the caged glutamate, we measured the kinetic constants for the channel opening of the GluR6 receptor.

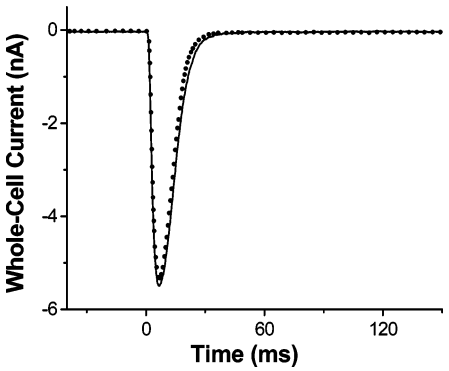

FIGURE 4: Test of the biological properties of the caged glutamate with the GluR6Q receptor expressed in HEK-293 cells. Superimposed were the whole-cell currents induced by 200 μM glutamate in the absence (line) and presence (solid circle) of 2 mM caged glutamate. The sampling frequency was 5 kHz. However, for clarity, the number of points shown in the solid-circle trace was reduced in various regions of the current trace.

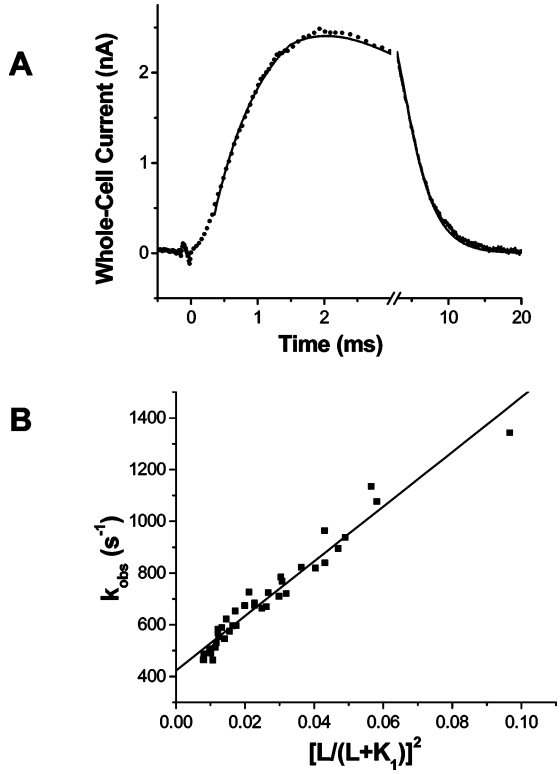

FIGURE 5: (A) Whole-cell current induced by the laser pulse photolysis of caged glutamate. A pulse of laser was fired at time zero. The concentration of glutamate released was estimated to be 200 μM using the cell-flow method (see Materials and Methods). The observed first-order rate constant, k_{obs}, of 1340 ± 35 s^{-1}, was obtained from the fitting of the rising phase according to eq 2. Note that the current is plotted in the direction opposite to that recorded. (B) Linear plot of k_{obs} as a function of glutamate concentration using eq 3. Each data point represents a k_{obs} obtained at a particular concentration of photolytically released glutamate. From this plot, k_{cl} and k_{op} were determined to be (4.2 ± 0.2) × 10^2 and (1.1 ± 0.4) × 10^4 s^{-1}, respectively.

The rising phase of the whole-cell current, as shown in Figure 5A, represents the channel opening, while the current fall is indicative of channel desensitization. A single-exponential rate law, shown in eq 2, adequately described >95% of the rising phase for all the concentrations of the photolytically liberated glutamate, ranging from 40 to 220 μM. This result is consistent with the assumption that the rate of ligand

binding is fast relative to channel opening (*21*). On the basis of this assumption, eq 3 can be derived to obtain the channel-opening (k_{op}) and channel-closing (k_{cl}) rate constants from the observed first-order rate constant (k_{obs}) as a function of ligand concentration.

$$I_t = I_A(1 - e^{-k_{obs}t}) \quad (2)$$

$$k_{obs} = k_{cl} + k_{op}\left(\frac{L}{L + K_1}\right)^2 \quad (3)$$

I_A is the maximum current amplitude, while I_t represents the current amplitude at time t. A k_{obs} corresponding to a glutamate concentration was determined using eq 2. Plotting k_{obs} versus $[L/(L + K_1)]^2$, shown in Figure 5B according to eq 3, yielded k_{cl} of $(4.2 \pm 0.2) \times 10^2$ s^{-1} and k_{op} of $(1.1 \pm 0.4) \times 10^4$ s^{-1}, respectively.

Eq 3 was derived assuming the rate of ligand binding is fast relative to that of channel opening. This assumption is plausible based on the experimental evidence (i) that a single-exponential rate process was observed that adequately described >95% of the rising phase of the receptor response and (ii) that a single-exponential rate law was all it required to describe the rising phase in all the concentrations of the photolytically liberated glutamate. The kinetic criteria described in (ii) would be preferably tested more thoroughly if the rising phase kinetics could be measured even at the concentration leading to saturation. However, this has not been technically feasible. To ensure that our measurement of the GluR6Q response was under the condition that ligand binding was fast, we paid special attention to our experiments at low concentrations of glutamate. This was because the ligand binding was a bimolecular process; thus, at sufficiently low concentrations of glutamate, ligand binding could eventually become rate limiting. The glutamate concentration of 40 μM was chosen as the lowest concentration at which we measured the rate of current rise, seen in Figure 5B. The 40 μM ligand concentration corresponded to the fraction of the channel in the open form being about 4%. This was the fraction at which the observed rate of the current rise was comparable to the rate of the channel closing, as determined for the nicotinic acetylcholine receptor (*21*) (see a detailed discussion in the companion paper). Therefore, the ligand concentration at this fraction should be already high enough to ensure that the ligand binding is fast or not limiting to the channel-opening rate process. Furthermore, the independent results from Heckmann and co-workers (*26*) in fact supported our assumption that the relatively slow channel-opening process, but not the preceding steps of ligand binding, was observed. The maximum rise time of ~220 μs that they obtained, under the ligand saturation condition (e.g., at 10 mM glutamate, reached by rapid flow measurement), was in close agreement with ours (see Discussion). From the maximum rise time, the channel-opening rate constant was postulated to be ~10 000 s^{-1}, again close to the value we report here. Therefore, these independent results affirmed our assumption that the kinetic rate process we measured reflected the rate of the channel opening rather than the ligand binding. This is important because eq 3, on which our kinetic analysis of the rising phase was based, is only valid when the channel opening is slow, as compared to the ligand binding.

In the analysis of the whole-cell current induced by the photolysis of caged glutamate shown in Figure 5A, the k_{obs} at a given glutamate concentration was obtained by fitting only the rising phase of the current using eq 2. The contribution of the current fall after the initial rise was negligible. This is because the rate of the current fall, which can be fitted by a single-exponential rate equation, was, on average, 3−4 times slower than the rate of the current rise in all the concentrations of glutamate in the laser−pulse photolysis measurement. In agreement to this observation, a single-exponential rate law could adequately describe >95% of the rising phase of the current, shown in Figure 5A. Moreover, the simultaneous fitting of both the rising and the falling phases by two first-order rate equations yielded a k_{obs} value that was identical, within a 5% error range, to the k_{obs} value obtained by the single fit. This analysis was valid at all glutamate concentrations. These results therefore demonstrate that the rising phase of the whole-cell current in a laser−pulse photolysis experiment can be measured and analyzed separately (i.e., without the complication of the desensitization reaction). Although the desensitization reaction may start concomitantly when the ligand binds (which would formally involve a transition to the states of desensitization from the closed and perhaps the open states), the observed rate of desensitization is slow, relative to the rate of channel opening. Thus, the degree of desensitization is insignificant at the time the peak current is reached, allowing the desensitization process to be effectively ignored in our analysis of the channel-opening kinetics. However, this kinetic analysis is valid only in the laser−pulse photolysis measurements. With the slower solution exchange methods, the rise time of the current may be lengthened due to a slow and/or an uneven rate of solution exchange to equilibrate ligand molecules with their binding sites. In this case, the channel activation and desensitization are mixed during the rise time of the current. Both the rate of rise of the current and the peak current amplitude are distorted by desensitization. The use of the laser−pulse photolysis technique, as shown in the present study, overcomes these problems. As a result, the channel-opening rate process can be measured as a kinetically distinct, separable rate process from the slow desensitization reaction.

DISCUSSION

In the present study, we focused on GluR6Q, a representative kainate receptor. The mechanism here established provides initial understanding of the time scale by which the GluR6Q channel operates as a function of glutamate concentration. Further, the comparison of the channel-opening kinetics yields quantitative description of the integrated synaptic signal if both GluR6Q and GluR2Q$_{flip}$ are colocalized and activated by glutamate at the same time.

Channel-Opening and -Closing Rate Constants. The channel-opening rate constant, $k_{op} = 11\,000$ s^{-1}, defines the time scale by which the GluR6Q channel opens, upon the binding of glutamate. This rate constant should represent the transition from the doubly liganded, closed-channel form to the open-channel form. Gouaux and Armstrong (*40*) previously proposed a structural model in which the bilobe closure is thought to link to the channel opening. It is therefore possible that the k_{op} reflects the dynamic process of lobe closure following ligand binding. The value of k_{op} indicates

that the $t_{1/2}$ value of the channel opening is less than 100 μs. This is consistent with the μs time scale by which the amino acid residues in the ligand-binding domain undergo motions, as observed by NMR spectroscopy (*41*). On the other hand, the channel-closing rate constant for GluR6Q, $k_{cl} = 420\ s^{-1}$, is a measure of how long a channel can stay open and thus reflects the lifetime of the open channel (*21*). The lifetime of an open channel can be alternatively characterized by a single-channel recording technique, but such studies of the glutamate-activated GluR6Q channel have not been yet reported. Swanson et al. (*9*) investigated the single-channel events initiated by a low concentration of domoate to the outside-out patches containing the GluR6Q receptor. Three conductance levels and two mean open times were observed. The mean open time of 2.3 ms for the minor component (23.8%) was in agreement with both the channel-closing rate constant from the present study and the deactivation rate constant by Heckmann et al. (*26*). However, the mean open time of 0.6 ms for the major component (76.2%) was not comparable to the results of either study and may be observed only in the presence of domoate. It is known, for instance, that glutamate- (*28*) and kainate-activated (*30*) AMPA receptors in hippocampal neurons have different channel-closing rate constants.

Channel-Opening Probability (P_{op}). The determination of the k_{cl} and k_{op} from the present study now enables the estimation of the channel-opening probability for the GluR6Q channel. P_{op} is defined as the rate constant for the forward reaction or the channel opening divided by the sum of the rate constants for the forward and backward or channel-closing reactions (i.e., $k_{op}/(k_{op} + k_{cl})$). It reflects the probability by which a channel can open once it is bound with ligand(s) (*21*, *27*, *42*). As such, P_{op} can be intuitively interpreted as a relative measure of how fast the channel opens, with respect to the rate of the channel closing. For instance, a P_{op} of 0.5 indicates that the channel opens as fast as it closes, whereas the P_{op} of 0.91 suggests that the channel can open 10 times faster, as compared to the rate of channel closing. A higher value of P_{op} like 0.91, for instance, further implies that the open-channel form is relatively more stable since the backward reaction or the channel-closing reaction is slow, as compared to the forward reaction or the channel-opening reaction. In other words, the fraction of the open-channel form under this quasi-equilibrium condition is high.

For the GluR6Q receptor, P_{op} was calculated to be 0.96 using the experimentally determined k_{op} and k_{cl}. This value is in agreement with a high probability of opening generally observed in recombinant AMPA and kainate receptors. However, for reasons not yet clear, the P_{op} obtained in the present study is higher than the P_{op} of 0.65 reported from the nonstationary variance analysis of the glutamate-induced channel conductance (*27*). In an attempt to address the discrepancy in the P_{op} value, it is helpful to consider the results from an independent study by Heckmann and co-workers (*26*). In that study, it was not possible to determine the k_{cl} and k_{op} directly. However, based on the maximum rise time of ~200 μs achieved at 10 mM glutamate, and on the assumption that $k_{cl} \ll k_{op}$, the k_{op} was estimated to be 10 000 s^{-1} (*26*). This value is comparable with the k_{op} measured in here by laser−pulse photolysis (11 000 s^{-1}). Using the 10 000 s^{-1} as k_{op}, a k_{cl} of 5400 s^{-1} would be estimated if the P_{op} were assumed to be 0.65. This is >10 times larger than our value (420 s^{-1}). Is it possible, then, that we may have significantly underestimated the k_{cl} from our measurement? Several lines of evidence seem not to support this possibility. First, as shown in Figure 4, the caged glutamate was not an inhibitor. Second, the k_{cl} for GluR2Q$_{flip}$, as presented in the preceding article, was ~7 times larger than that for GluR6Q. This comparison suggests that the photolysis of the caged glutamate did not limit the rate of the current rise for the GluR6Q and thus the determination of the k_{cl}. Third, as we discussed earlier, the desensitization could not have contributed appreciably during the current rise so as to distort its rate. Taken together, these results suggest that the magnitude of the k_{cl} determined in this study should reflect or closely reflect the rate of channel closing.

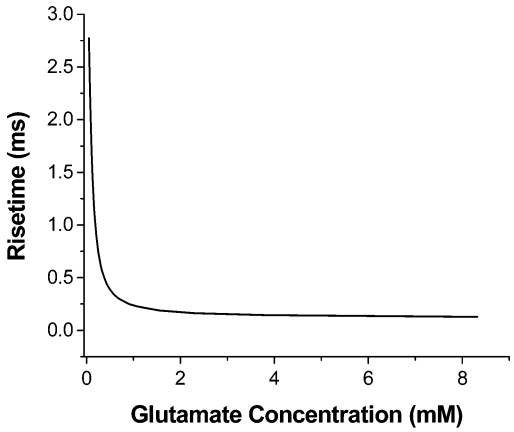

FIGURE 6: Time course of the GluR6Q channel opening as a function of glutamate concentration. A rise time was obtained from the calculation of a k_{obs} value using a first-order rate law for the progression of the reaction between 20 and 80% current amplitudes. The k_{obs} value as a function of glutamate concentration corresponded to the fitted value from the experimentally determined k_{cl} and k_{op} for GluR6Q.

A P_{op} value as high as 0.9 has been in fact observed in the studies of other ligand-gated ion channels. For instance, earlier studies of a nicotinic acetylcholine receptor by single-channel recording reported a P_{op} of 0.98, defined as the ratio of the mean open time to the sum of the mean open and mean closed time (in which k_{op} or $\beta = 30\ 600\ s^{-1}$ and k_{cl} or $\alpha = 714\ s^{-1}$, respectively) (*42*). This value was in agreement with the P_{op} of 0.94, obtained by the measurement of k_{op} and k_{cl} (*21*). Furthermore, the P_{op} for the γ-aminobutyric acid receptor ($GABA_A$) was reported to be 0.98 from the k_{op} and k_{cl} obtained from the laser−pulse photolysis approach (*43*). This value is roughly comparable to the P_{op} of 0.90 obtained by using the rapid solution exchange method with the outside-out patches containing the same receptor (*62*). In the latter study, the macroscopic current response was used directly to calculate the P_{op} since the $GABA_A$ receptor desensitizes ~16-fold slowly, as compared to the GluR6Q receptor, under the ligand saturation condition.

Time Course of the Channel Opening. With the k_{cl} and k_{op} values obtained for the GluR6Q, the time course for the channel opening can be further defined. The rise time is used to represent the time course of the channel opening and is described by k_{obs}, which is determined by a single-exponential rate equation, based on the measured k_{cl} and k_{op} values. The rise time depends on the concentration of ligand and further takes the rate of the channel closing into account. As shown in Figure 6, the rise time decreases, as expected with an

increasing concentration of ligand. However, when the ligand concentration is very low, the ligand binding may become rate limiting. The k_{obs} value will then reflect the rate of ligand binding rather than the channel opening. Under this circumstance, the rise time will be less sensitive to the change of ligand concentration, a phenomenon previously observed with the muscle nicotinic acetylcholine receptor (*44*). When the ligand concentration reaches 5 mM or higher, the rise time becomes invariant, as seen in Figure 6. This is predicted by eq 3: when $L \gg K_1$, the k_{obs} is the sum of k_{cl} and k_{op} and no longer depends on L (since the receptor is saturated by bound glutamate). Consequently, the rise time is the shortest, registering at 120 μs. This value is similar to the one previously estimated by Heckmann et al. (*26*). In essence, 120 μs represents the fastest observed time by which the GluR6Q channel can open. In fact, the maximum k_{obs}, described previously, can be estimated by k_{op} alone since $k_{op} \gg k_{cl}$.

Comparison of the Channel-Opening Rate Constants with Other Receptors. The k_{op} of 11 000 s^{-1} for the GluR6 homomeric receptor channel is comparable to the k_{op} of 9400 s^{-1} for the muscle type nicotinic acetylcholine receptor (*21*) and the k_{op} of 9500 s^{-1} for the AMPA receptors expressed in hippocampal neurons (*28*). The k_{cl} of 420 s^{-1} is slightly smaller than the k_{cl} of either 580 s^{-1} for the muscle type nicotinic acetylcholine receptor (*21*) or 640 s^{-1} for the kainate-activated AMPA receptors (*30*) but considerably smaller than the k_{cl} of 1100 s^{-1} for the glutamate-activated AMPA receptors in hippocampal neurons (*28*). However, the k_{cl} and k_{op} for GluR6Q are about 6- and 7-fold smaller, respectively, as compared to the homomeric $GluR2Q_{flip}$ AMPA channel (*25*).

It may be surprising that the channel-opening kinetic constants of GluR6Q, in comparison to those of $GluR2Q_{flip}$, are significantly different, given that kainate and AMPA receptors have similar molecular biology and topologies (*1*, *6*), bilobed ligand-binding domains (*40*, *45*−*47*), and pore regions (*48*, *49*). Both receptors also desensitize rapidly (*1*). However, kainate and AMPA receptors do have some distinct properties. For example, kainate can bind and activate not only the GluR6 kainate receptor but also other kainate receptors as well as AMPA receptors (*50*−*52*). AMPA, however, is incapable of activating the GluR6 receptor (*3*), although it can be effective on the selective combination of GluR6 with other kainate receptor subunits, such as GluR6Q/KA-2 (*9*). Recent structural studies have revealed that amino acid residues, which are located at the subunit interface (*40*) and are critical in determining AMPA receptor desensitization (*45*, *53*), are not conserved in kainate receptors. Furthermore, kainate receptors have a larger, more polar subsite G (a part of the ligand binding site), as compared to AMPA receptors (*54*). In addition, kainate receptors have different amino acid residues in the vicinity of the γ-substituent of an agonist bound to the receptor, such as glutamate, AMPA, and kainate (*54*). Mutation of one of these residues, asparagine 686 in GluR6, for instance, rendered this receptor sensitive to AMPA (*15*) and (*S*)-5-iodowillardine (*55*). Taken together, if the channel opening is related to the lobe closure as suggested by Gouaux and Armstrong (*40*), the difference between the kinetics of GluR6 and GluR2 arises at least in part from differences in the rate of lobe closure induced by the binding of glutamate.

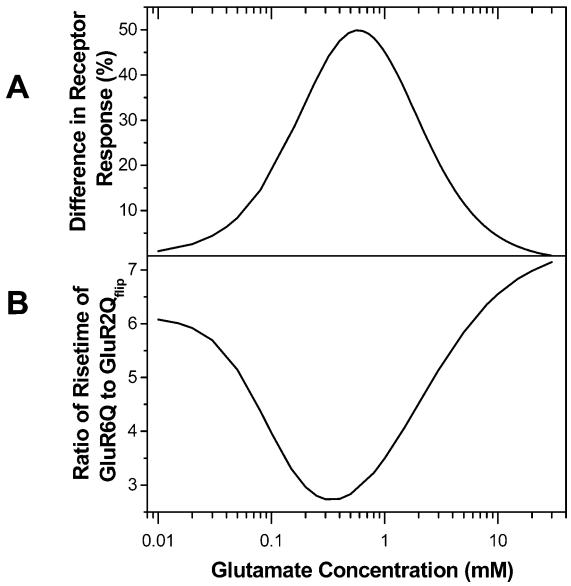

FIGURE 7: (A) Difference of the dose−response relation between GluR6Q (Figure 3A) and $GluR2Q_{flip}$ (Figure 3A in the companion paper). In both cases, the relative whole-cell response was set to 100%. Therefore, the difference seen in this figure represents a maximum of 100%. (B) Ratio of the rise time of GluR6Q (Figure 6) to $GluR2Q_{flip}$ (Figure 7 in the companion paper). The definition of the rise time was given in the text.

To highlight the comparison of the channel-opening kinetic properties for these two receptors, the difference of the receptor response as a function of glutamate concentration (panel A) and the ratio of the rise time (panel B) are displayed in Figure 7. The interpretation of the results shown in Figure 7 may be most meaningful if it is assumed that the $GluR2Q_{flip}$ and GluR6Q receptors colocalize and function at a postsynapse in response to a common chemical signal, glutamate. Clearly, the difference between the receptor responses to glutamate is a result of more than a 2-fold difference between the K_1 values (or roughly the EC_{50} values). This difference is the largest when the concentration of the glutamate is around 0.6 mM and then disappears when the concentration is saturating. Because the K_1 value for the GluR6Q is smaller (0.45 vs 1.27 mM for $GluR2Q_{flip}$), a higher fraction of the GluR6Q receptor channels open at concentrations of glutamate below 0.6 mM. As the glutamate concentration continues to rise, the fraction of the $GluR2Q_{flip}$ channels begins to increase. At saturating concentration, both channels can fully open, as seen the disappearance of this difference in Figure 7A. Furthermore, the difference in the channel-opening rate constant as a function of the glutamate concentration leads to the difference in the rise time for the opening of the receptor channel, seen in Figure 7B. The GluR6Q opens slowly, because of its smaller k_{op}, as compared to $GluR2Q_{flip}$. When the glutamate concentration is low (see the lower end of the plot in Figure 7B), the ratio indicates that the rise time, reflective of the channel-closing rate constant, is about 6-fold longer for the GluR6Q channel. However, as the glutamate concentration increases, the major current component will be the slow, GluR6Q response. In contrast, when the glutamate concentration becomes higher than 0.3 mM, the fast, $GluR2Q_{flip}$ channel will become more and more dominant. If these results are indicative of how the $GluR2Q_{flip}$ and GluR6Q receptors function at a postsynapse (where kainate and AMPA receptors are known to colocalize) (*56*), then at lower glutamate concentrations, it

is expected that the integrated neuronal signal will be slow and mostly GluR6Q-like; the AMPA receptors are virtually nonfunctional. At higher glutamate concentrations, the function of AMPA receptors becomes prominent, resulting in a faster rise of the integrated signal. In this case, the fast phase is due to the opening of the $GluR2Q_{flip}$ channel, whereas the slow phase is attributed to the GluR6Q channel. These predictions are particularly meaningful given the fact that both channel types have a similar desensitization rate at a given glutamate concentration and the channel-opening probability values are the same (i.e., 0.96). Furthermore, our predictions may explain the previous observations that the excitatory postsynaptic currents (EPSC) in thalamocortical axons (*57*) and in hippocampal neurons (*58*) show a fast AMPA receptor-dependent component and a slower one, mediated by the activation of kainate receptors.

Characterization of the Channel-Opening Kinetics by Macroscopic Receptor Current. The measurement of the GluR6Q channel-opening kinetics, based on the glutamate-induced macroscopic current, has been made possible by using the laser−pulse photolysis technique with a time resolution of ~60 μs. This fine resolution is required to resolve the opening of the channel from the ensuing, rapid desensitization reaction. Piezoelectrical perfusion devices, which are considered as the most rapid, direct ligand application method, have a time resolution in the range of 200−400 μs for solution exchange (*1*). The laser−pulse photolysis technique, therefore, represents an alternative approach, with an improved time resolution by at least 3−4-fold. This technique is useful to characterize channel-opening kinetics in general. It may be particularly useful to determine the lifetime of the open channels for both kainate and AMPA subtypes because the use of glutamate, an endogenous neurotransmitter, in single-channel recordings is often prohibitive, due to the rapid receptor desensitization following the glutamate binding. Consequently, other activating ligands such as domoate, which induces the nondesensitizing kainate receptor response, are used instead. Furthermore, some channel-modifying reagents such as concanavalin A, which also induces the nondesensitizing kainate receptor response, are applied together with glutamate. In the former case, the kinetic constants for channel opening are known to be markedly different (*28*, *30*). In the latter case, the use of additional, modifying reagents complicates the understanding of the true kinetic properties of the receptor of interest since the mechanism of action of these reagents themselves remains to be elucidated (*2*).

Since the first demonstration of its use in the kinetic investigation of the channel-opening mechanism for the muscle type nicotinic acetylcholine receptor (*21*), the laser−pulse photolysis technique has been applied to several other receptor types (*28*, *30*, *43*). It has further enabled kinetic investigations of the mechanism of drug−receptor interactions in the μs-to-ms time region where the receptors were in the functional forms prior to receptor desensitization (*20*, *59*−*61*). It is now possible to explore, with a time resolution of ~60 μs, the structure and function relationship and the role of an individual subunit in heteromeric receptor complexes. Furthermore, the mechanism of regulation for this homomeric receptor channel by inhibitors can be also elucidated. The inhibitors for the GluR6Q receptor, for instance, may become candidates of antiepileptic drugs.

ACKNOWLEDGMENT

We thank Dr. Steve Heinemann (Salk Institute) for the GluR6Q cDNA. We are grateful to Drs. Vasanthi Jayaraman (University of Texas at Houston) and Christof Grewer (University of Miami) for helpful discussions in setting up the laser. We thank Ming Xu for preparing some plasmids used in the study.

REFERENCES

1. Dingledine, R., Borges, K., Bowie, D., and Traynelis, S. F. (1999) *Pharmacol. Rev. 51*, 7−61.
2. Lerma, J., Paternain, A. V., Rodriguez-Moreno, A., and Lopez-Garcia, J. C. (2001) *Physiol. Rev. 81*, 971−98.
3. Egebjerg, J., Bettler, B., Hermans-Borgmeyer, I., and Heinemann, S. (1991) *Nature 351*, 745−8.
4. Egebjerg, J., and Heinemann, S. F. (1993) *Proc. Natl. Acad. Sci. U.S.A. 90*, 755−9.
5. Bennett, J. A., and Dingledine, R. (1995) *Neuron 14*, 373−84.
6. Wo, Z. G., and Oswald, R. E. (1994) *Proc. Natl. Acad. Sci. U.S.A. 91*, 7154−8.
7. Hollmann, M., Maron, C., and Heinemann, S. (1994) *Neuron 13*, 1331−43.
8. Burnashev, N., Zhou, Z., Neher, E., and Sakmann, B. (1995) *J. Physiol. 485*, 403−18.
9. Swanson, G. T., Feldmeyer, D., Kaneda, M., and Cull-Candy, S. G. (1996) *J. Physiol. (London) 492*, 129−42.
10. Bowie, D., and Mayer, M. L. (1995) *Neuron 15*, 453−62.
11. Bernard, A., and Khrestchatisky, M. (1994) *J. Neurochem. 62*, 2057−60.
12. Vissel, B., Royle, G. A., Christie, B. R., Schiffer, H. H., Ghetti, A., Tritto, T., Perez-Otano, I., Radcliffe, R. A., Seamans, J., Sejnowski, T., Wehner, J. M., Collins, A. C., O'Gorman, S., and Heinemann, S. F. (2001) *Neuron 29*, 217−27.
13. Porter, R. H., Eastwood, S. L., and Harrison, P. J. (1997) *Brain Res. 751*, 217−31.
14. Rubinsztein, D. C., Leggo, J., Chiano, M., Dodge, A., Norbury, G., Rosser, E., and Craufurd, D. (1997) *Proc. Natl. Acad. Sci. U.S.A. 94*, 3872−6.
15. Swanson, G. T., Gereau, R. W. T., Green, T., and Heinemann, S. F. (1997) *Neuron 19*, 913−26.
16. Trussell, L. O., and Fischbach, G. D. (1989) *Neuron 3*, 209−18.
17. Hess, G. P. (1993) *Biochemistry 32*, 989−1000.
18. Niu, L., Grewer, C., and Hess, G. P. (1996) *Chemical kinetic investigations of neurotransmitter receptors on a cell surface in a microsecond time region*, Vol. VII, Acadamic Press, New York.
19. Hess, G. P., and Grewer, C. (1998) *Methods Enzymol. 291*, 443−73.
20. Niu, L., and Hess, G. P. (1993) *Biochemistry 32*, 3831−5.
21. Matsubara, N., Billington, A. P., and Hess, G. P. (1992) *Biochemistry 31*, 5507−14.
22. Wieboldt, R., Gee, K. R., Niu, L., Ramesh, D., Carpenter, B. K., and Hess, G. P. (1994) *Proc. Natl. Acad. Sci. U.S.A. 91*, 8752−6.
23. Chen, C., and Okayama, H. (1987) *Mol. Cell Biol. 7*, 2745−52.
24. Hamill, O. P., Marty, A., Neher, E., Sakmann, B., and Sigworth, F. J. (1981) *Pflugers Arch. 391*, 85−100.
25. Li, G., Pei, W. M., and Niu, L. (2003) *Biochemistry 42*, 12358−12366.
26. Heckmann, M., Bufler, J., Franke, C., and Dudel, J. (1996) *Biophys. J. 71*, 1743−50.
27. Traynelis, S. F., and Wahl, P. (1997) *J. Physiol. 503*, 513−31.
28. Li, H., Nowak, L. M., Gee, K. R., and Hess, G. P. (2002) *Biochemistry 41*, 4753−9.
29. Jonas, P., Major, G., and Sakmann, B. (1993) *J. Physiol. 472*, 615−63.
30. Jayaraman, V. (1998) *Biochemistry 37*, 16735−40.
31. Koike, M., Tsukada, S., Tsuzuki, K., Kijima, H., and Ozawa, S. (2000) *J. Neurosci. 20*, 2166−74.
32. Loftfield, R. B., and Eigner, E. A. (1969) *Science 164*, 305−8.
33. Colquhoun, D., and Ogden, D. C. (1988) *J. Physiol. 395*, 131−59.
34. Clements, J. D., Feltz, A., Sahara, Y., and Westbrook, G. L. (1998) *J. Neurosci. 18*, 119−27.
35. Rosenmund, C., Stern-Bach, Y., and Stevens, C. F. (1998) *Science 280*, 1596−9.

36. Safferling, M., Tichelaar, W., Kummerle, G., Jouppila, A., Kuusinen, A., Keinanen, K., and Madden, D. R. (2001) *Biochemistry 40*, 13948−53.
37. Mayer, M. L., Olson, R., and Gouaux, E. (2001) *J. Mol. Biol. 311*, 815−36.
38. Raymond, L. A., Blackstone, C. D., and Huganir, R. L. (1993) *Nature 361*, 637−41.
39. Paternain, A. V., Rodriguez-Moreno, A., Villarroel, A., and Lerma, J. (1998) *Neuropharmacology 37*, 1249−59.
40. Armstrong, N., and Gouaux, E. (2000) *Neuron 28*, 165−81.
41. McFeeters, R. L., and Oswald, R. E. (2002) *Biochemistry 41*, 10472−81.
42. Colquhoun, D., and Sakmann, B. (1985) *J. Physiol. 369*, 501−57.
43. Jayaraman, V., Thiran, S., and Hess, G. P. (1999) *Biochemistry 38*, 11372−8.
44. Franke, C., Hatt, H., Parnas, H., and Dudel, J. (1991) *Biophys. J. 60*, 1008−16.
45. Stern-Bach, Y., Bettler, B., Hartley, M., Sheppard, P. O., O'Hara, P. J., and Heinemann, S. F. (1994) *Neuron 13*, 1345−57.
46. Armstrong, N., Sun, Y., Chen, G. Q., and Gouaux, E. (1998) *Nature 395*, 913−7.
47. Paas, Y. (1998) *Trends Neurosci. 21*, 117−25.
48. Kuner, T., Beck, C., Sakmann, B., and Seeburg, P. H. (2001) *J. Neurosci. 21*, 4162−72.
49. Panchenko, V. A., Glasser, C. R., and Mayer, M. L. (2001) *J. Gen. Physiol. 117*, 345−60.
50. Kiskin, N. I., Krishtal, O. A., and Tsyndrenko, A. (1986) *Neurosci. Lett. 63*, 225−30.
51. Patneau, D. K., Vyklicky, L., Jr., and Mayer, M. L. (1993) *J. Neurosci. 13*, 3496−509.
52. Stern-Bach, Y., Russo, S., Neuman, M., and Rosenmund, C. (1998) *Neuron 21*, 907−18.
53. Partin, K. M., Bowie, D., and Mayer, M. L. (1995) *Neuron 14*, 833−43.
54. Jin, R., Horning, M., Mayer, M. L., and Gouaux, E. (2002) *Biochemistry 41*, 15635−43.
55. Swanson, G. T., Green, T., and Heinemann, S. F. (1998) *Mol. Pharmacol. 53*, 942−9.
56. Frerking, M., Malenka, R. C., and Nicoll, R. A. (1998) *Nat. Neurosci. 1*, 479−86.
57. Kidd, F. L., and Isaac, J. T. (1999) *Nature 400*, 569−73.
58. Frerking, M., and Ohliger-Frerking, P. (2002) *J. Neurosci. 22*, 7434−43.
59. Niu, L., Abood, L. G., and Hess, G. P. (1995) *Proc. Natl. Acad. Sci. U.S.A. 92*, 12008−12.
60. Grewer, C., and Hess, G. P. (1999) *Biochemistry 38*, 7837−46.
61. Jayaraman, V., Usherwood, P. N., and Hess, G. P. (1999) *Biochemistry 38*, 11406−14.
62. von Beckerath, N., Adelsberger, H., Parzefall, F., Franke, C., and Dudel, J. (1995) *Pfluegers Arch. 429*, 781−8.

BI034797T